

What perturbs NGC 2188?

H. Domgörgen¹, M. Dahlem^{2**}, R.-J. Dettmar³

¹ Sternwarte der Universität Bonn, Auf dem Hügel 71, D-53121 Bonn, Germany

² Space Telescope Science Institute, 3700 San Martin Drive, Baltimore, MD 21218, USA

³ Astronomisches Institut der Ruhr-Universität Bochum, Universitätsstr. 150, D-44780 Bochum, Germany

Received, Accepted

Abstract. VLA HI observations of the dwarf irregular galaxy NGC 2188 show that the gas and stars have spatial distributions which are substantially different. One end of the optical disk is strongly gas deficient, while neutral gas extends into the halo over distances of more than 2 kpc from the midplane. This and the peculiar velocity field suggest that NGC 2188 is a perturbed system, although it is not obviously an interacting galaxy.

In addition, NGC 2188 is remarkable for its interstellar disk-halo connection. An H α image of NGC 2188 shows the presence of spectacular features of ionized gas extending from a large star-forming complex up to 500 pc into the halo. Also, peculiar HI filaments and at least one superbubble are present in NGC 2188.

Key words: ISM: bubbles - Galaxies: halos - Galaxies: individual: NGC 2188 - (*Galaxies*): intergalactic medium - Galaxies: ISM - Galaxies: irregular

1. Introduction

Dwarf irregular galaxies are ideal laboratories to study the feedback processes between star formation and the interstellar medium (ISM). Due to their low mass and hence low gravity, young massive stars are able to blow large holes into the surrounding ISM (e.g. Holmberg II, Puche et al. 1992) and galactic winds are thought to play a major role in the evolution of dwarf galaxies (Marlowe et al. 1995, and references therein). The structures produced are longlived since differential rotation is hardly important.

Powerful tools to study the impact of massive stars on the ISM are H α images (showing the distribution of

Send offprint requests to: H. Domgörgen

* Partly based on observations obtained at ESO/La Silla (Chile)

** Affiliated with the Astrophysics Division in the Space Science Department of ESA

star-forming regions) and HI imagery (showing the superbubble expansion). The galaxies NGC 4449 (Bajaja et al. 1994), IC 10 (Shostak & Skillman 1989), and Sextans A (Skillman et al. 1988) are just some examples that HI synthesis maps are also necessary to understand the full nature of dwarf irregular galaxies (Skillman 1994).

NGC 2188 is an edge-on ($i \sim 86^\circ$) Magellanic type irregular galaxy (Tully 1988). Its absolute blue magnitude, $M_B \sim -17.87$ mag which is based on a distance of 7.9 Mpc (Tully 1988) indicates that its size is somewhere between those of dwarf galaxies and normal spirals. Although NGC 2188 was not detected in CO (Israel 1995), the measured colour index, $U - B = -0.21$, hints at the presence of a population of young stars.

As part of a project to investigate the interstellar disk-halo connection of nearby galaxies we obtained observations of NGC 2188. Here we present a detailed study of NGC 2188 based on a H α image as well as high resolution HI data. To our surprise we discovered large scale asymmetries between the optical and radio image of the galaxy. Additionally, huge gas structures extending from the disk into the halo were found.

2. Observations and data reduction

2.1. HI line data

HI data of NGC 2188 were collected with the VLA¹ synthesis telescope during two observing runs of 5 h each in October 1994 (CnB array) and a third run of 3.5 h in January 1995 (DnC array), filling in short baselines in order to obtain good sensitivity for extended emission.

The individual data sets were calibrated in a standard fashion with the AIPS software package. 3C147 was used as primary flux calibrator and 0616-349 for the phase calibration. After calibration all data of both arrays were combined. The final data set has a resolu-

¹ The VLA is a facility of the National Radio Astronomy Observatory, which is operated by Associated Universities, Inc., under contract with the National Science Foundation

tion of $11''.9 \times 11''.2$. After the continuum subtraction the maps showing line emission were CLEANed. Using uniform weighting, 512×512 pixel maps with a pixel size of $3''.5$, a resolution of $12''$, and an rms noise of 1.3 mJy/beam were produced. Applying natural weighting we also created maps with a resolution of $25''$ and an rms noise of 0.3 mJy/beam . Both map versions are used in the analysis: the uniform weighted maps for investigations of small scale structures, and the natural weighted maps for investigating extended structures. The velocity resolution of our data is 5.18 km s^{-1} .

2.2. Optical narrow band imaging

$\text{H}\alpha$ images of NGC 2188 were obtained in Feb. 1993 with the ESO 2.2m telescope on La Silla, using EFOSC2 (Melnick et al., 1989) with a 1024×1024 pixel Thompson CCD chip. The spatial scale is $0''.34/\text{pixel}$; the seeing during our observations was $\simeq 0''.9$, which gives a linear resolution of 34 pc. The integration times were 2×30 min with the $\text{H}\alpha$ filter #694, which has a $FWHM$ of 61 \AA and a central wavelength of $\lambda_0 = 6557 \text{ \AA}$, and 10 min with Gunn r .

The data reduction was performed using the IRAF software package. Bias and dark were subtracted and gain variations were removed using dome flatfields. We performed the continuum subtraction using the scaled R-band image (e.g., Dettmar 1990).

3. Data analysis and results

3.1. HI line emission from NGC 2188

Using the channel maps, a “moment analysis” was performed, applying the so-called “unsharp masking” technique with a 3σ significance level for blanking.

3.1.1. HI content and distribution

The total HI line flux of NGC 2188 in our data is $S_{HI} = 20.4 \pm 0.6 \text{ Jy km s}^{-1}$. Assuming the typical case of small optical depth, this corresponds to an HI gas mass of $3 \times 10^8 \text{ M}_\odot$. Using the Parkes telescope Reif et al. (1982) found $S_{HI} = 32.9 \text{ Jy km s}^{-1}$ for NGC 2188. Thus, $\sim 38\%$ of the total flux might be missed by the VLA measurements due to missing short spacings, or NGC 2188 could be surrounded by a halo of low surface brightness HI gas below our current detection limit of $1.6 \times 10^{20} \text{ cm}^{-2}$. However, this discrepancy is uncertain, because the Reif et al. measurements are of low S/N.

Superimposed on the $\text{H}\alpha$ frame of NGC 2188 we present in Figure 1 contours of the total HI line flux density. The disk of NGC 2188 is well defined by a high surface brightness ridge. Column densities reach peak values of $4.8 \times 10^{21} \text{ cm}^{-2}$ and drop rapidly along the minor axis. A comparison of the HI contours and the $\text{H}\alpha$ distribution shows an overall correspondence of the HI high surface brightness disk and the star forming disk. Note that the

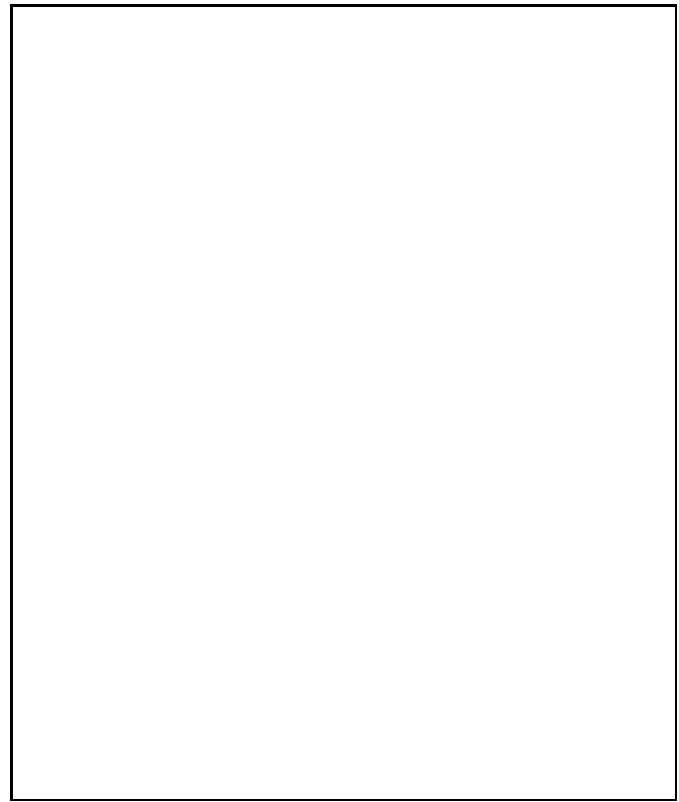


Fig. 1. $\text{H}\alpha$ image of NGC 2188 with overlying HI contours. Contour levels are: $2.5, 7.5, \dots, 47.5 \times 10^{20} \text{ cm}^{-2}$.

position angle of the $\text{H}\alpha$ disk does not stay constant over the whole disk. Instead we find the disk to be slightly bent to the east near both ends of the $\text{H}\alpha$ emission distribution, leading to a “banana”-shape.

The disk is surrounded by an extended envelope of neutral gas which is distributed asymmetrically with respect to the disk: HI emission corresponding to a column density of $2.4 \times 10^{20} \text{ cm}^{-2}$ can be found $\sim 2.7 \text{ kpc}$ east of the midplane and $\sim 1.6 \text{ kpc}$ to the west (Fig. 1).

Intensity profiles along the minor axis of NGC 2188 can be approximated with a Gaussian component (representing the beam-smeared disk emission) plus two wings of emission extending further out. In order to get a rough estimate of the percentage of emission coming from this extended component we produced a representative intensity profile along the minor axis in the declination range $-34^\circ 04' 33'' > \delta > -34^\circ 06' 53''$ (thus avoiding contributions from the peculiarly bent outer ends of the disk). Subtracting a Gaussian profile from the resulting emission distribution we find that the residual corresponds to $\sim 30\%$ of the emission.

Figure 2 shows a superposition of the HI map of NGC 2188 on a digitized POSS plate. Here one can note another peculiarity of this galaxy. While there is plenty of neutral gas extending perpendicular to the disk in places where we do not find optical continuum emission, we find

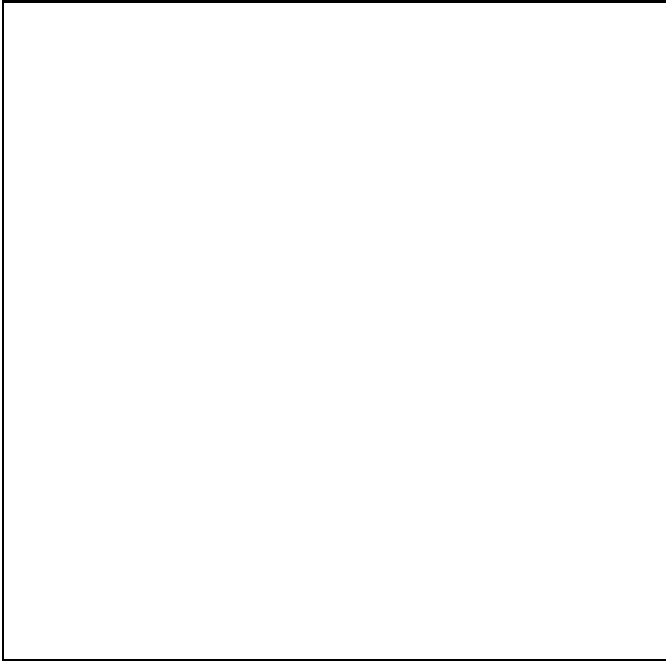


Fig. 2. Superposition of the HI data of NGC 2188 on a digitized POSS plate. Contour levels are: $2.5, 7.5, \dots, 47.5 \times 10^{20} \text{ cm}^{-2}$.

optical continuum (i.e., stellar light) in the disk plane at the northern end of the disk where no HI emission could be detected.

Imbedded into the low surface brightness emission surrounding the disk of NGC 2188, HI filaments at higher surface brightness can be found emerging from the disk and extending into the halo.

One very prominent feature extending ~ 1.8 kpc perpendicular to the galaxy's disk is located south-west of the disk at $\alpha, \delta(2000) = 06^h 10^m 08^s, -34^\circ 07' 20''$. The position-velocity (*pv*) diagram in Figure 3.a shows that the radial velocity of this "worm" increases with distance from the plane. The velocity difference compared to the underlying disk reaches up to $\sim 25 \text{ km s}^{-1}$.

Two other spur-like HI structures east of the disk close to the center of the galaxy, can be shown to be connected to a superbubble expanding in the area where the two features leave the disk ($\alpha, \delta(2000) = 06^h 10^m 0.5, -34^\circ 06' 18''$). Figure 3.b shows a *pv*-diagram along the minor axis at $\delta(2000) = -34^\circ 06' 18''$. Thus the velocity structure of the gas between the two HI "spurs" is displayed. The velocity spread of the HI gas shows clear signatures of bubble expansion with an expansion velocity of about $v = 10 \text{ km s}^{-1}$. The radius of the bubble is $15''$ (575 pc) and its flux is about 0.7 Jy km s^{-1} corresponding to $6 \times 10^6 \text{ M}_\odot$. Following Heiles (1979), an energy of $1.6 \times 10^{53} \text{ erg}$ is needed to produce a structure with these properties.

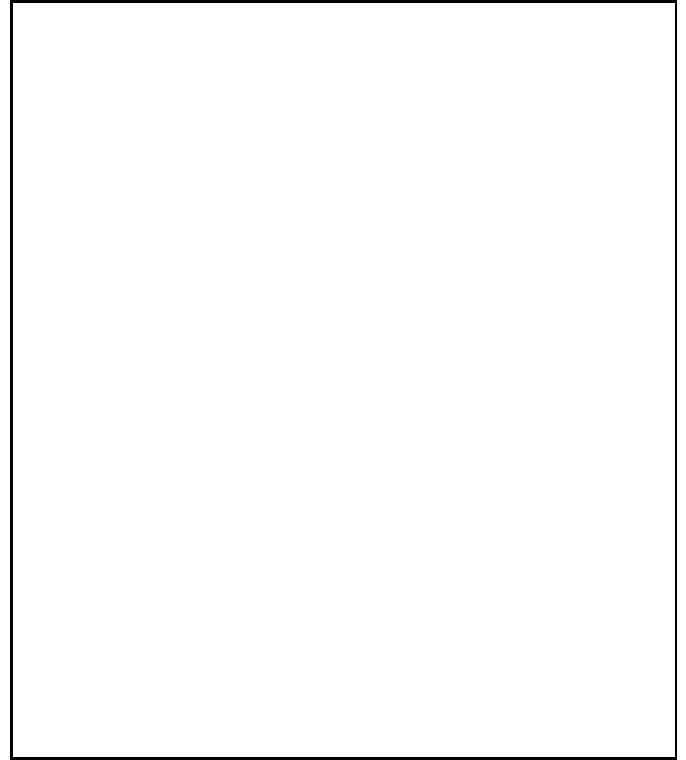


Fig. 3. Position-velocity diagrams parallel to the minor axis of NGC 2188: Cut through **a.** the southernmost filament; **b.** the superbubble east of the disk and close to the center of NGC 2188. Contour levels are $2, 4, \dots, 16 \text{ mJy/beam}$.

3.1.2. The velocity field

Figure 4 displays a contour plot of the intensity weighted HI velocity field of NGC 2188 superposed on its grey scale representation. In order to emphasize the large scale structure of the velocity field, we present the natural weighted version of the data (25" resolution). In the northern half of the disk of NGC 2188 the velocity field is that of a highly inclined rotating disk. In the halo east of the disk the velocity contours bend towards north. However, in the southern half of the disk as well as the halo, the velocity contours are very irregular. This is especially true for that part of the galaxy where the most prominent HI filament extends from the disk into the halo (§ 3.2.1). For $\delta < -34^\circ 08'$ the velocity gradient follows the disk bending to the east. Independent of the peculiar gas distribution (see above), these kinematic disturbances also indicate a large-scale perturbation of the neutral gas in NGC 2188.

Figure 5 shows a *pv*-diagram along position angle 0. This is nearly but not exactly equivalent to a *pv*-diagram along the major axis of NGC 2188 due to the bent shape of the galaxy's disk. The inner $1.5'$ of the disk are rotating rigidly. At $\sim \delta = -34^\circ 05' 30''$ and at $\sim \delta = -34^\circ 07' 00''$ signs for the onset of differential rotation can be found. However, it is quite hard to describe the *pv*-diagram just by rigid and differential rotation.

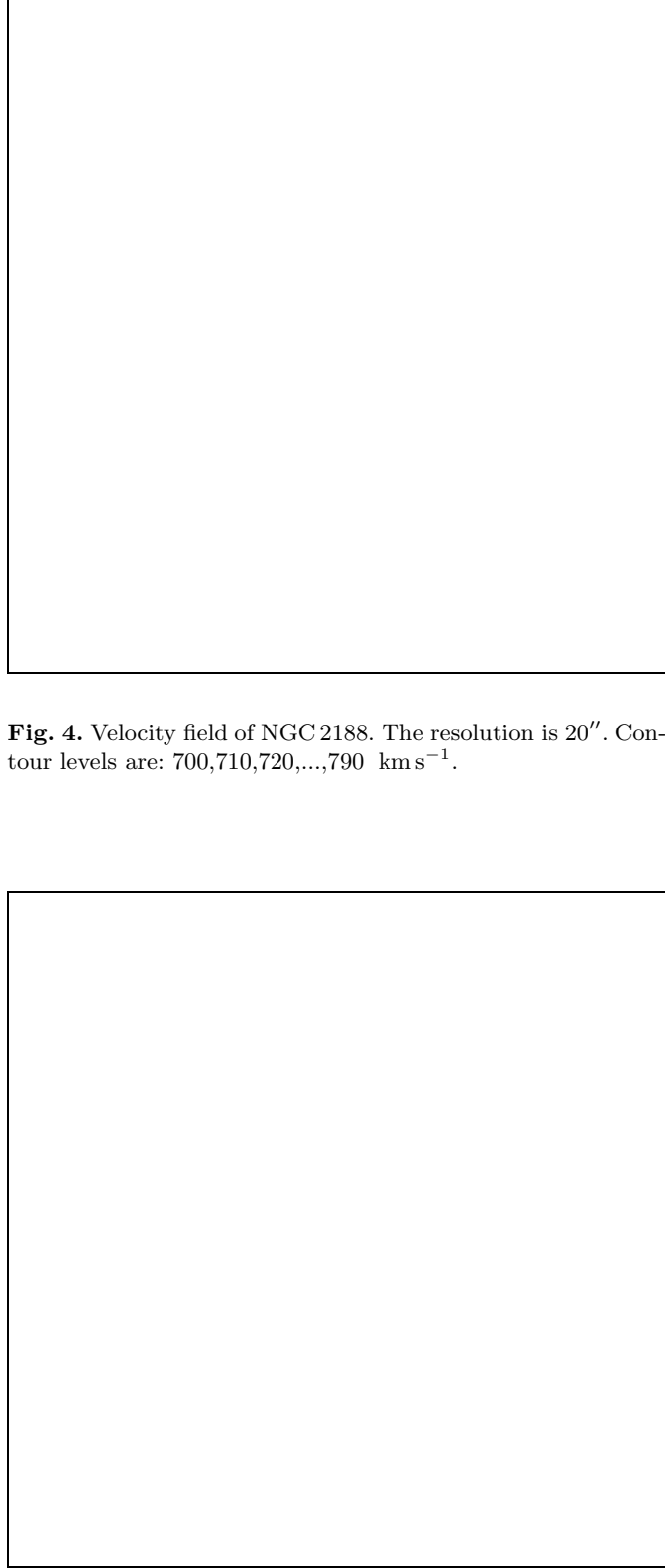


Fig. 4. Velocity field of NGC 2188. The resolution is $20''$. Contour levels are: $700, 710, 720, \dots, 790 \text{ km s}^{-1}$.

From the HI spectrum of NGC 2188 we determine the velocity width at a 20% level to be 145 km s^{-1} . This is consistent with what we find from Figure 5 and allows us (in combination with the radius for rigid rotation) a rough estimate of the total mass in the inner 3.5 kpc radius of NGC 2188. We find $M_{\text{tot}} \sim 2.1 \times 10^9 M_{\odot}$.

3.2. The structure of the ionized gas in NGC 2188

In Figure 1 we display our continuum subtracted $\text{H}\alpha$ image of NGC 2188.² The star formation activity which is mostly concentrated in the south of NGC 2188, in a region 2 kpc across along the major axis, is asymmetric with respect to the galaxy centre. Probably the most spectacular features on the $\text{H}\alpha$ image are the prominent emission line filaments. These start in the most conspicuous star formation regions in the disk and extend up into the halo of NGC 2188. Their lengths range from ~ 150 pc up to ~ 500 pc, while their typical width is only ~ 40 pc. Most of the filamentary emission is found west of the disk. The southern HII region complex is also surrounded by an extended envelope of diffuse emission line gas with a thickness of ~ 350 pc.

A comparison of the HI contours and the $\text{H}\alpha$ distribution shows an overall correspondence of the HI high surface brightness disk and the star forming disk. The disk has a “banana”-shaped appearance, as already noted for the HI distribution.

4. Discussion and conclusions

4.1. NGC 2188: a perturbed galaxy

The most surprising result of the investigation of the neutral gas in NGC 2188 is the large number of irregularities and asymmetries which are present in the data. All these peculiarities, i.e., 1) the “banana” shape of the disk, 2) the asymmetric distribution of gas around the main body of NGC 2188, 3) the excess optical continuum emission in the northern half of the disk, and 4) the disturbed velocity field of NGC 2188 suggest a large-scale (possibly external) disturbance.

NGC 2188 is a member of a small group of only three galaxies (Tully 1988). Its closest neighbour (ESO 364–29) has a systemic velocity only 42 km s^{-1} higher than that of NGC 2188, but its projected distance to NGC 2188 is 180 kpc and it is even smaller than NGC 2188 itself. If we assume a relative velocity of the two galaxies of 200 km s^{-1} , nearly 2×10^9 years (~ 8 rotation periods) must have passed since their closest passage. A relative velocity of 200 km s^{-1} is somewhat higher than $129 \pm 22 \text{ km s}^{-1}$,

² Note that while we will be speaking about “ $\text{H}\alpha$ ”, a contribution of about $\sim 20\%$ to the line emission comes from the $\lambda\lambda 6548/6583\text{\AA}$ [NII] lines. No correction for this has been applied.

Fig. 5. Position-Velocity diagram along position angle 0° at $\alpha = 6^h 10^m 9\text{s}.9$. Contour levels are: $24, 36, 48, \dots, 600 \text{ mJy/beam}$.

the “square root of the average squared rms radial velocity of the galaxies in a group with respect to its average system velocity” determined for 18 loose groups of galaxies by Williams and Rood (1987). Thus, it seems unlikely that the peculiar gas distribution of NGC 2188 can be explained by an interaction with that galaxy.

The shape of the disk of NGC 2188 as well as the HI distribution are both reminiscent of bow shock phenomena as seen in galaxies moving into a tenuous intracluster gas (e.g. Cayatte et al. 1994) and the large scale disturbances of NGC 2188 can coherently be explained by gas stripping processes due to an intergalactic medium. In order to investigate if this is a viable process (although NGC 2188 is not a member of a galaxy cluster) we will now estimate a lower limit for the density of a possible intragroup medium. There are basically two processes by which an intergalactic medium can remove gas from a galaxy: ram pressure stripping and stripping due to transport processes.

In the case of ram pressure by the intergalactic medium the ram pressure has to be higher than the local surface gravity of the interstellar gas: $\rho_{\text{IGM}} v^2 > 2\pi G \sigma_{\text{tot}} \sigma_{\text{gas}}$ (Gunn & Gott 1972). ρ_{IGM} is the density of the intergalactic medium. σ_{tot} and σ_{gas} are the total surface densities and the gas surface density respectively. They can be estimated from the HI data. σ_{tot} we calculate from the maximum velocity and the corresponding radius to be $2.2 \times 10^8 \text{ M}_\odot \text{ kpc}^{-2}$. σ_{gas} we estimate assuming that the HI mass in the disk of NGC 2188 is distributed evenly over the HI disk area which has a radius of $\sim 4.3 \text{ kpc}$. We take only the disk gas ($2 \times 10^8 \text{ M}_\odot$) under consideration and get $\sigma_{\text{gas}} = 3.4 \times 10^6 \text{ M}_\odot \text{ kpc}^{-2}$. Finally, we again assume $v \sim 200 \text{ km s}^{-1}$ for the velocity of NGC 2188 perpendicular to its plane. All these assumptions yield $\rho_{\text{IGM}} > 5 \times 10^{-3} \text{ cm}^{-3}$.

Transport processes can cause stripping of gas with a rate that in some cases exceeds that caused by ram pressure stripping (Nulsen 1982). Nulsen found that the mass loss rate of a galaxy due to thermal conduction and viscous stripping can be expressed as $\dot{M} = \pi r^2 v \rho_{\text{IGM}}$. We assume that the amount of mass lost by NGC 2188 is comparable to the fraction of disk gas that resides in an area comparable to the northern gas deficient part of NGC 2188. This area is roughly equivalent to a quarter of a ring with a thickness of 1.7 kpc ($0.76'$). Using σ_{gas} from above, we obtain $M > 4.7 \times 10^7 \text{ M}_\odot$. For mass loss timescales longer than half a rotation period of NGC 2188 a gas deficiency should be observed over the entire galaxy. Therefore, a reasonable timescale for the mass loss probably is half a rotation period of NGC 2188 ($\sim 1.2 \times 10^8 \text{ years}$). Using $r = 4.3 \text{ kpc}$ and $v = 200 \text{ km s}^{-1}$ we find $\rho_{\text{IGM}} \sim 1 \times 10^{-3} \text{ cm}^{-3}$.

Consequently, if the appearance of NGC 2188 is due to gas stripping processes ρ_{IGM} has to be at least $1 \times 10^{-3} \text{ cm}^{-3}$. This is comparable to the densities of the intergalactic medium in galaxy clusters (Sarazin 1992). Since

NGC 2188 is not a cluster member it seems unlikely to us that the morphology of NGC 2188 is due to gas stripping processes.

However, it is possible that NGC 2188 interacted or is interacting with an intergalactic HI cloud. In this scenario, both the peculiar gas dynamics and the absence of a visible (stellar) interaction partner could be explained. In fact, the morphology of the neutral gas in NGC 2188 strongly reminds of similar features in IC 10 where they have been interpreted as an interaction with an HI plume (Shostak & Skillman 1989).

4.2. The disk-halo connection of NGC 2188

Having HI as well as H α data available also allows us to study the interstellar disk-halo connection of NGC 2188. NGC 2188 is certainly remarkable for its prominent features of diffuse ionized gas (DIG). Figure 1 shows that there is a clear correlation between star formation processes in the disk and the occurrence of DIG in the halo of NGC 2188. The HI data show also that peculiar filaments of neutral gas extending from the disk into the halo of NGC 2188 exist. Similar to the HI features in NGC 3079 (Irwin 1990) these filaments can be interpreted in terms of Heiles shells. Then their presence suggests that superbubble expansion is an important process for the disk-halo interaction of NGC 2188.

Comparing the HI and the H α data we do not find a correlation between DIG filaments and superbubble features. In particular the giant superbubble east of the center of NGC 2188 does not show prominent DIG emission. This is unlikely to be due to dust absorption, since NGC 2188 is a late type galaxy and since the HI features are found above the disk where the column densities are low. The absence of such a correlation can very well be explained by an age sequence: during the lifetime of an OB superassociation diffuse ionized structures are produced in its vicinity and expand into the halo of the galaxy where densities are lower. As the cluster ages the ionized structures recombine quickly. However, HI structures which have been formed due to the combined energy input of stellar winds and supernovae can still be observed even when all the diffuse H α emission has vanished.

Acknowledgements. We are thankful to the NRAO for providing their facilities during the process of data reduction. We also thank E. Brinks, E.D. Skillman and K.S. de Boer for useful discussions. H.D. was supported by the DFG Graduiertenkolleg Magellansche Wolken and additional travel support was granted under De 385/8-1. This research has made use of the NASA/IPAC Extragalactic Database (NED), which is operated by the Jet Propulsion Laboratory, Caltech, under contract with the National Aeronautics & Space Administration.

References

Bajaja E., Huchtmeier W.K., Klein U., 1994, A&A 285, 385
Cayatte V., Balkowski C., 1994, AJ 107, 1003

Dettmar R.-J., 1990, A&A 232, L15
 Gunn, J.E., Gott, J.R., 1972, ApJ 176,1
 Heiles C., 1979, ApJ 229, 533
 Irwin J.A., Seaquist, E.R. 1990, ApJ 353, 469
 Israel F.P., Tacconi L.J., Baas F., 1995, A&A 295, 599
 Marlowe A.T., Heckman T.M., Wyse R.F.G., Schommer R.,
 1995, ApJ 438, 563
 Melnick J., Dekker H., D'Odorico S., 1989, ESO Operating
 Manual No. 4
 Nulsen P.E.J., 1982, MNRAS 198, 1007
 Puche D., Westpfahl D., Brinks E., Roy J.-R., 1992, AJ 103,
 1841
 Reif K., Mebold U., Goss W.M., van Woerden H., Siegman B.,
 1982, A&AS 50, 451
 Sarazin C.L. in *Clusters and Superclusters of Galaxies*, Ed.
 A.C. Fabian, Cambridge University Press Vol. 366
 Shostak G.S., Skillman E.D. 1989, A&A 214, 33
 Skillman E.D., Terlevich R., Teuben P.J., von Woerden H.,
 1988, A&A 198, 33
 Skillman E.D., 1994 in *Violent Star Formation from 30 Do-
 radus to QSO's*, Ed.: G. Tenorio-Tagle. Cambridge Univer-
 sity Press, 168
 Tully R.B., 1988, "Nearby Galaxies Catalog", Cambridge Uni-
 versity Press
 Williams B.A., Rood H.J., 1987, ApJS 63, 265